PAPER

Dissipative stability and dynamical phase transition in two driven interacting qubits

To cite this article: K V Shulga 2024 *Quantum Sci. Technol.* **9** 025021

IOP Publishing Quantum Sci. Technol. 9 (2024) 025021 https://doi.org/10.1088/2058-9565/ad34f6

Quantum Science and Technology

RECEIVED
22 December 2023

REVISED
8 March 2024

ACCEPTED FOR PUBLICATION
18 March 2024

PUBLISHED
26 March 2024

PAPER

Dissipative stability and dynamical phase transition in two driven interacting qubits

K V Shulga

International Center for Elementary Particle Physics, The University of Tokyo, 7-3-1 Hongo, Bunkyo, Tokyo 113-0033, Japan

E-mail: kirill_shulga@protonmail.ch

Keywords: quantum dynamics, dissipative stability, entanglement phenomena, floquet quantum systems, dynamic phase transitions, quantum computing

Abstract

We examine a two-qubit system influenced by a time-periodic external field while interacting with a Markovian bath. This scenario significantly impacts the temporal coherence characteristics of the system. By solving the evolution equation for the density matrix operator, we determine the characteristic equilibration time and analyze the concurrence parameter-a key metric for quantifying entanglement. Our findings reveal the system's ability to navigate through a dynamic phase transition. These results pave the way to designing systems of interacting qubits demonstrating robust entanglement under realistic conditions of interaction with the environment.

1. Introduction

Quantum computing aims to harness quantum-mechanical phenomena, such as entanglement and superposition of states, to create highly efficient systems of interconnected qubits that could outperform classical computers [1]. Recent years have witnessed successful implementations of quantum computation principles in systems featuring multiple qubits. Within this context, various studies have advocated using driven qubits as a strategy for stabilization [2, 3]. The scalability of coherently interacting qubits is pivotal for achieving efficient fault-tolerant quantum computation. Nevertheless, this endeavor presents formidable challenges, including the need to address quantum nonlinearity and coherence suppression or absence, both integral to quantum computation [4–7].

The interaction of quantum systems with their environment emerges as a primary source of decoherence and dephasing, introducing equilibration and phase-kicks to the system [8, 9]. Consequently, dissipation stands out as a formidable obstacle in realizing quantum computing devices. Addressing this challenge has become a current trend, focusing on mitigating the adverse effects of dissipation mechanisms in systems featuring multiple coupled qubits. The complexity inherent in many-body dissipative-driven dynamics poses a significant hurdle.

This emphasis on mitigating dissipation aligns with the broader exploration of coherent quantum dynamics in systems subject to a time-periodic external perturbation, known as *Floquet quantum systems* [10–12]. Extensive attention has been devoted to experimental and theoretical studies in this realm. The investigation of periodically driven quantum systems, composed of many interacting quantum particles, promises a wider variety of temporal interference patterns [13–17]. Predictions include the emergence of diverse non-equilibrium coherent quantum phases and quantum phase transitions in spatially extended Floquet quantum systems [13, 14, 18, 19]. These phases are characterized by a broken temporal-translation symmetry induced by the underlying time-periodic perturbation and exhibit enhanced quantum entanglement.

In recent years, numerous experimental studies on Floquet systems, known as time crystals, have emerged [20–25]. They provide valuable insights into nonequilibrium dynamics subjected to periodic Hamiltonians. In particular, many showed the possibility of experimentally demonstrating the emergence of discrete time-crystalline order in arrays of many spins.

We focus on a minimal system of two coupled qubits based on a model introduced in [26] to establish a foundation for such investigations. This model is designed to elucidate the emergence of phenomena related to temporal coherence in a small number of qubits. Our analysis calculates the equilibration time, highlighting the formation of a dynamic phase transition induced by dissipation. Additionally, we examine the formation and decay of entanglement, employing concurrence as a key metric. This research provides valuable insights into understanding dissipative driven dynamics in quantum systems, potentially laying the groundwork for future advancements in the design and optimization of quantum computing devices.

2. Model

Let us consider a series of interacting qubits that are subjected to periodic spin-flip pulses controlled by a Floquet Hamiltonian:

$$H(t) = \begin{cases} \frac{\alpha}{2}\sum_i \sigma_i^x, & 0 < t < t_1 \\ g\sum_{\langle i,j\rangle}\left(\sigma_i^x\sigma_j^x + \sigma_i^y\sigma_j^y\right), & t_1 < t < T, \end{cases} \tag{1}$$

where $\sigma_i^{(x,y)}$ are Pauli matrices of the ith qubit, T is the period of Floquet modulation, g is the qubit interaction strength, and α is the normalized amplitude of the periodic flip pulses and close to the π-pulse, so $\alpha t_1 = \pi - 2\varepsilon$, where ε is the detuning from ideal π-pulse. When selecting parameters for our system, we fix the excitation energy of one qubit to unity, allowing all other constants to be defined in terms of it.

We model dissipative processes using the Lindblad master equation (here and after that $\hbar = 1$):

$$\frac{\mathrm{d}\rho}{\mathrm{d}t} = L[\rho] = -i[H(t),\rho] + \sum_k \gamma_k\left(A_k\rho A_k^\dagger - \frac{1}{2}\left\{A_k^\dagger A_k, \rho\right\}\right), \tag{2}$$

where ρ is the density matrix of the qubit system, and the sum over dissipation channels k consists of the jump operators A_k with the rates $\gamma_k = \{\gamma_i^+, \gamma_i^-, \gamma_i^d\}$, where the i index denotes the qubit number. We consider two main sources of decoherence that are typical for qubit experiments. The first of them is a coupling to a thermal bosonic bath modeled by the operators $A_i^\pm = \sigma_i^\pm$ (where $\sigma_i^\pm = (\sigma_i^x \pm \sigma_i^y)/2$) with dissipation rates $\gamma_i^- = g_1(1 + n\mathrm{th})$ and $\gamma_i^+ = g_1 n\mathrm{th}$, where g_1 is the coupling strength between the qubit and the bath, and nth is the thermal distribution of the external bath. The second source of decoherence is the dephasing, modeled by the operator $A_i^d = \sigma_i^z$ with $\gamma_i^d = g_2$.

To model the system's evolution, we use a vectorized density matrix to calculate a discrete time-periodic Liouville superoperator. This dynamical map applied to the initial quantum state $|\uparrow\uparrow\ldots\uparrow\rangle$ representing a ferromagnetic configuration of spins. When qubits in interaction are coupled to a thermal environment, the system's dynamics are influenced, causing a gradual relaxation toward thermal equilibrium. This, in turn, results in a reduction of the system's entanglement, a phenomenon observable through various parameters including total polarization, entanglement entropy, purity, and concurrence, as illustrated in figure 1.

Various parameters of the system exhibit distinct responses to the presence of coupling with the thermal environment. With an increase in the Floquet cycle number, the system's state becomes more mixed, as evidenced by the shift of the total polarization toward zero, as illustrated in figures 1(a) and (c). Simultaneously, the entanglement entropy S experiences an increase, signifying the system's enhanced mixing. This augmentation of a mixed state diminishes the quantum correlations between subsystems, reducing information that can be gleaned about the system's state through measurements of individual subsystems. Intriguingly, the concurrence C, considered a measure of two-qubit entanglement (see appendix A), decreases as the system becomes more mixed. The concurrence parameter stands out as a superior metric for characterizing entanglement in dissipative systems compared to negativity and other potential parameters. It offers a precise measure of entanglement between qubits, allowing for a clear distinction between separable and entangled states. This distinction is crucial for understanding the dynamics of entanglement and its resilience against environmental influences in the studied system. Notably, a critical Floquet cycle value exists, beyond which the concurrence reaches zero, and this critical point is proportional to $1/\gamma_k$, as depicted in figure 1(b) and (d). This paper establishes a foundation for comprehending the dissipative dynamics of phase transitions and the coherence properties inherent in such quantum systems.

To investigate the variation of concurrence with increasing coupling strength between the two-qubit system and the thermal bath, we select a parameter set closely resembling those achievable in real experiments, with the ratio g_1/g_2 fixed (see appendix B). This ratio may vary within wide permissible ranges; however, such variations do not affect the outcomes claimed in the article.

We assume the thermal energy is much smaller than the qubit energy gap and explore the persistence and formation of entanglement quantified by concurrence. In figure 2, we illustrate the dynamics of concurrence

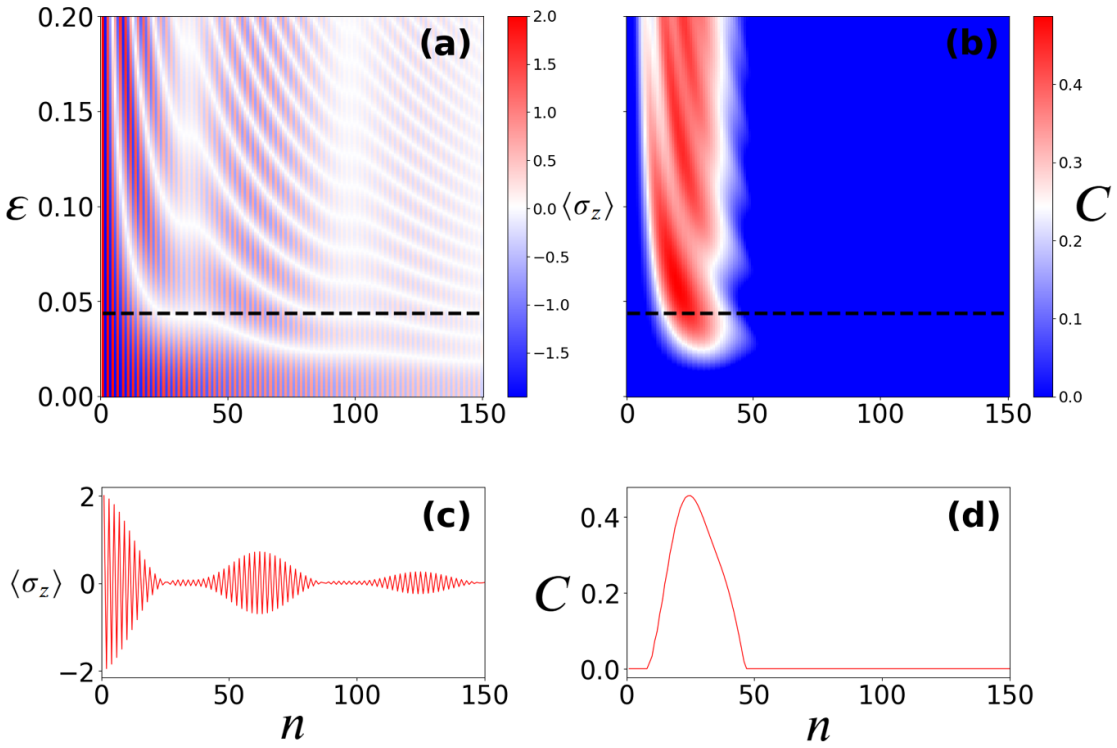

Figure 1. (a) Instantaneous total polarization $\langle\hat{\sigma}_z\rangle$ and (b) concurrence as a function of the discrete-time n and the pulse imperfection ε for two interacting qubits. The detuning $\delta_{1,2}$ between the qubits is set to zero. (c) and (d) Cross-sections of the plots in (a) and (b) at $\varepsilon = 0.0436$ indicated with dashed lines. Except as otherwise noted $g_1 T = 0.01$, $g_2 T = 0.0025$, $n\text{th} = 0.08$, $gT = 0.05$.

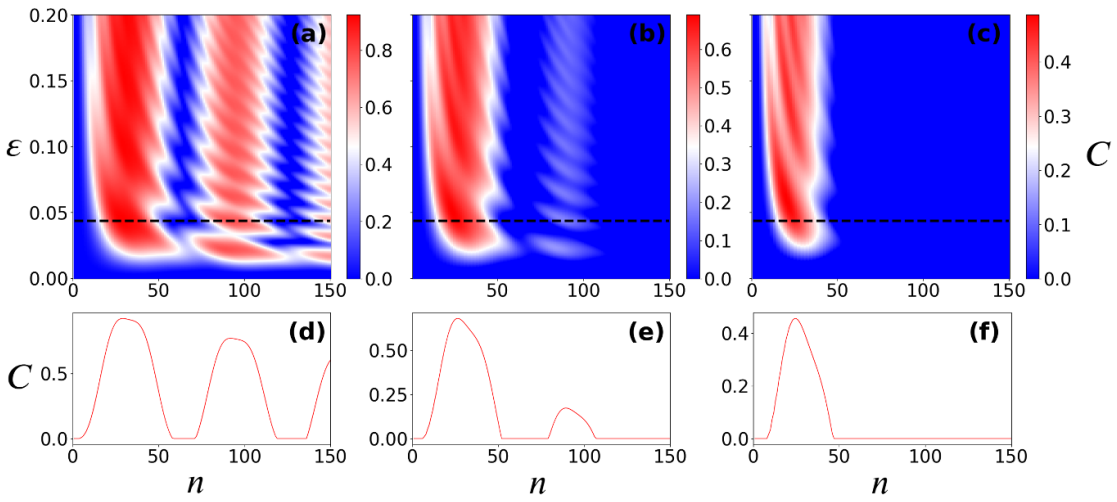

Figure 2. (a)–(c) Concurrence as a function of the discrete-time n and the pulse imperfection ε for two interacting qubits. The detuning $\delta_{1,2}$ between the qubits is set to zero. (d)–(f) Cross-sections of the plots in (a)–(c) at $\varepsilon = 0.0436$ indicated with dashed lines. Ratio $g_1/g_2 = 4$, $n\text{th} = 0.08$, $gT = 0.05$ for all plots, $g_1 T = 0.001$ in (a) and (d), $g_1 T = 0.005$ in (b) and (e), $g_1 T = 0.01$ in (c) and (f).

starting from zero-entanglement initial conditions for different values of ε. Notably, with an increase in the coupling strengths g_1 and g_2 between the qubits and the thermal bath, the amplitude of the concurrence oscillations decreases.

Our model can be validated using a real experimental setup, such as a small superconducting processor comprising transmon qubits, as demonstrated in works [20, 25]. The parameters utilized in our calculations were inspired by typical values of relaxation and dephasing times, the durations of control pulses in modern transmon qubits, and their coupling strengths. The code is available at [27].

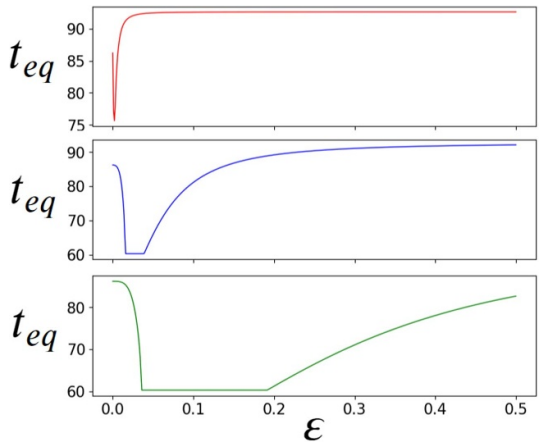

Figure 3. Dependence of the equilibration time $t_{\rm eq}$ on detuning ε at different interaction strength, red $gT = 0.001$, blue $gT = 0.02$, green $gT = 0.1$. $g_1 T = 0.01$, $g_2 T = 0.0025$, nth $= 0.08$, $gT = 0.05$.

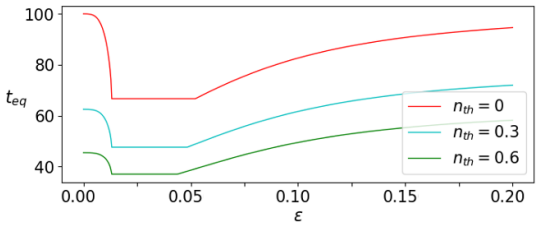

Figure 4. Dependence of the equilibration time $t_{\rm eq}$ on detuning ε at different temperatures of the bath nth. Red nth $= 0$, cyan nth $= 0.3$, green nth $= 0.6$. $g_1 T = 0.01$, $g_2 T = 0.0025$, nth $= 0.08$, $gT = 0.05$.

3. Results

Both local observables and concurrence are determined through numerical solutions of (2). To ascertain the characteristic lifetime of the system, or the *dissipative equilibration time*, we employ a numerical diagonalization approach on the vectorized representation of the Lindbladian superoperator (2), obtaining the set of eigenvalues λ_i. The superoperator spectral gap, denoted as $\Delta_1 = -\max(\mathrm{Re}\lambda_i)$, is defined as the smallest distance from the imaginary axis to an eigenvalue of L, serving as the basis for calculating the equilibration time $t_{\rm eq} = 1/\Delta_1$. By equilibration time, we mean that, after initial transients, the expectation value of the quantity in question exhibits slight fluctuations around its average value over an infinite time, thus being very close to this saturation point in most cases. This scale indicates the time during which quantum computations can be performed without occurrence of overwhelming errors.

After a characteristic dissipation time, entanglement vanishes, while oscillations of local observables remain stable and detectable for an extended period, as depicted in figures 1(a) and (c). This result holds significant implications for quantum computing implementations: even as local time-coherence persists, entanglement may already be lost, rendering computations infeasible. Additionally, we explore the connection between the $t_{\rm eq}$ regimes and concurrence.

The equilibration time, representing the system's operational lifetime is depicted as a function of the detuning parameter in figure 3.

The dependence reveals three distinct regimes: decreasing $t_{\rm eq}$, constant $t_{\rm eq}$, and increasing $t_{\rm eq}$. The emergence of a constant $t_{\rm eq}$ region is linked to the transition from a weakly interacting regime to the region of large ε. The transition from the decreasing to constant $t_{\rm eq}$ regime exhibits extreme sharpness in the weak interacting regime. However, the transition from the constant to an increased $t_{\rm eq}$ regime is smoother.

The parameter region characterized by a constant $t_{\rm eq} = \mathrm{const}$ proves particularly intriguing for the study and comprehension of dissipative systems. Within this region, the constant equilibration time $t_{\rm eq}$ value diminishes with an increase in bath temperature, as illustrated in figure 4. Moreover, the boundary values of ε, which delineate this region, changes under the influence of temperature (weakly) and the interaction strength g between the two qubits, as shown in figure 5.

Our observations reveal that the first transition point shifts closer to $\varepsilon = 0$ with decreasing dissipation strength, while the second transition point remains unchanged, maintaining a value of $\varepsilon_{\rm crit} = gT$.

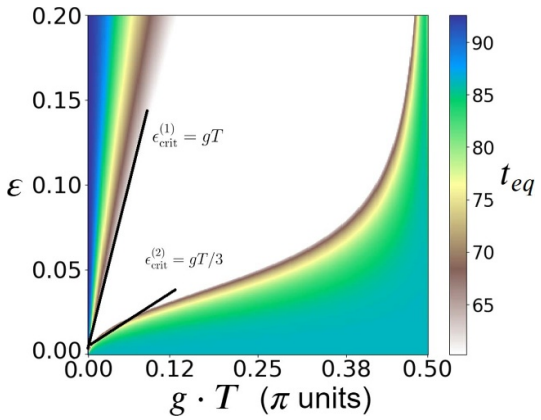

Figure 5. Decreasing, stable (white), and increasing lifetime regimes in the control parameter space. Two black lines indicate $\varepsilon = gT/3$, and $\varepsilon = gT$ transition asymptotics. $g_1 T = 0.01$, $g_2 T = 0.0025$, $n\text{th} = 0.08$, $gT = 0.05$.

Since the system operates far from equilibrium, the parametric behavior of the dynamical order parameter $1/t_{\rm eq}$ signifies a dynamical phase transition. As depicted in figure 5, this figure illustrates the three regimes within the complete parametric space, characterized by growth, reduction, or stability against changes in ε. In the weak coupling regime, the transitions follow simple relations, specifically $\varepsilon^{(1)}_{\rm crit} = gT$ and $\varepsilon^{(2)}_{\rm crit} = gT/3$. However, as we move away from this limit, the diagram reveals a significant complexity in dynamics, underscoring the intricate behavior of a system comprised of only two interacting qubits (see appendix C).

Hence, the upper limit of $\varepsilon^{(1)}_{\rm crit}$ holds limited interest in the context of practical experiments with qubits. This is because a non-ideal control pulse value comparable to the coupling constant is relatively rare. In contrast, the lower limit $\varepsilon^{(2)}_{\rm crit}$ serves as a crucial demarcation between two phases. One phase represents a stable yet short-lived region, wherein fluctuations of parameters exert minimal influence on the final time of quantum entanglement disappearance. The other phase encompasses a region where qubits can sustain entanglement for a more extended period, but external fluctuations have the potential to alter this duration. We posit that the stability exhibited by the region with $t_{\rm eq} = \text{const}$ could be leveraged to enhance contemporary quantum algorithms. Our findings underscore the significance of robust entanglement, exemplified by the stability observed in the region with constant $t_{\rm eq}$, highlighting its potential to enhance the reliability of quantum algorithms.

4. Conclusion

In conclusion, our study has demonstrated that a dissipative system comprising two qubits under periodic Floquet pumping may exhibit a loss of quantum entanglement, as quantified by concurrence, despite yielding observables indistinguishable from those in the non-dissipative scenario. Furthermore, our analysis of the equilibration time has revealed distinct regions, with particular emphasis on the intriguing $t_{\rm eq} = \text{const}$ region. Notably, within this region, the disappearance of coherence persists with an unchanged minimum time, spanning a wide parameter range. This finding underscores the intricate interplay between qubit interactions, Floquet modulations, and dissipation—a phenomenon crucial for various quantum computing applications. Even in the case of just two qubits, the behavior of such systems can manifest complexity. This paper establishes a foundational understanding of the coherence properties and dissipative dynamical phase transitions inherent in these systems, paving the way for further exploration and development in quantum information processing.

Data availability statement

All data that support the findings of this study are included within the article (and any supplementary files).

Acknowledgments

We thank Ihor Vakulchyk and Mikhail Fistul for useful discussions and Toshiaki Inada for proofreading the article.

Appendix A. Concurrence of two interacting qubits

Concurrence is a measure of the degree of entanglement between two qubits. Hill and Wootters introduced it [28] in 1997 as an alternative to the von Neumann entropy of entanglement [29] for the characterization of the entanglement between two qubits.

The concurrence is defined as follows: consider a two-qubit state represented by the density matrix ρ. Then, define the matrix $\tilde{\rho} = (\sigma_y \otimes \sigma_y)\rho^*(\sigma_y \otimes \sigma_y)$, where σ_y is the Pauli matrix acting on the y-axis and ρ^* is the complex conjugate of ρ in the standard basis. The concurrence of the state ρ is then given by

$$C(\rho) = \max(0, \lambda_1 - \lambda_2 - \lambda_3 - \lambda_4), \tag{3}$$

where λ_i are the eigenvalues of the non-Hermitian matrix $R = \sqrt{\sqrt{\rho}\tilde{\rho}\sqrt{\rho}}$, sorted in decreasing order.

One of the advantages of the concurrence over the von Neumann entropy of entanglement is that it can be extended to mixed states. In particular, for a mixed state ρ, the concurrence is defined as the convex roof of the concurrence of the pure state decompositions of ρ. This allows for more accurate characterization of the entanglement in realistic scenarios, where the system's state is typically mixed.

Moreover, the concurrence has a simple geometric interpretation: it is related to the distance of the state ρ to the set of separable states. In particular, a state is separable if and only if its concurrence is zero. Therefore, the concurrence provides a clear criterion for identifying entangled states.

Appendix B. Selecting the ratio between g_1 and g_2

The Kramers–Kronig [30, 31] relation is a fundamental result in optics, condensed matter physics, and other fields, connecting the real and imaginary parts of the complex response function. In the context of quantum information, the Kramers–Kronig relation is often invoked in the analysis of qubits relaxation and dephasing times, which are typically characterized by the parameters T_1 and T_2, respectively. The Kramers–Kronig relation provides an upper bound on T_1 in terms of T_2, given by $T_1 \leqslant 2T_2$.

Interestingly, this inequality becomes an equality in the limit where the spectral density of the noise is a Lorentzian function (Kubo's formula [32]). In this case, the dynamics of the qubit can be described by the Bloch–Redfield master equation [33, 34], which contains two coupling constants, g_1 and g_2, corresponding to the relaxation and dephasing processes, respectively. In the Kramers–Kronig limit, these coupling constants become related by $g_1 \geqslant \sqrt{2}g_2$. In our paper, we work with a slightly larger relaxation rate that satisfies this inequality, which is much more common in experiments with real qubits.

This result has important implications for engineering qubits with long coherence times. In particular, it suggests that reducing the dephasing rate g_2 may not necessarily improve T_1, and vice versa. Rather, a delicate balance between these two processes must be maintained to achieve optimal qubit performance. Understanding this balance is crucial for designing and operating future quantum devices, and the Kramers–Kronig relation provides a powerful tool for analyzing and optimizing their performance.

Appendix C. Complex behavior of different equilibration time regions

We explored the positions of three distinct regions concerning the behavior of equilibration time in the parameter space of ε and g over a wide range. This dependence exhibits periodic behavior, with discernible shifts in the system's dynamics at very large coupling values, see figure 6. Within the $t_{eq} = const$ region, the emergence of slender dotted lines is notable, and the intermittency of these lines intensifies with decreasing bath temperature. These lines are double, representing a sudden increase and subsequent return to the initial constant value of equilibration time within a very narrow range of parameters. Intriguingly, these artifacts vanish entirely at zero temperature. The mechanism underlying the appearance of additional segments of such lines remains an interesting puzzle for us, warranting further investigation and exploration.

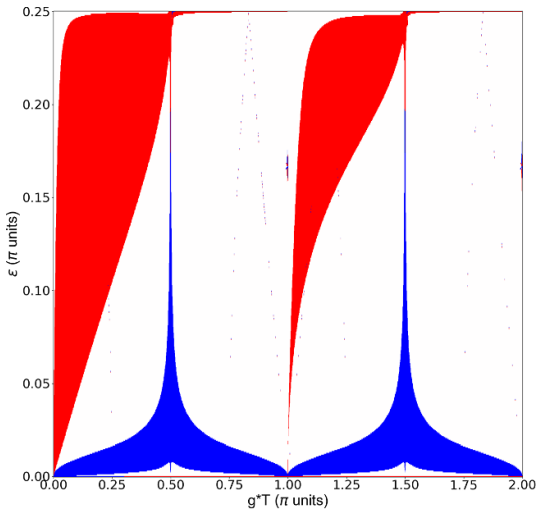

Figure 6. Diagram of equilibration time regions in a wide range of epsilon and g parameters. Three regions are highlighted, increasing (red), decreasing (blue) and constant (white) time. Periodicity is visible, as well as artifacts appearing in the form of broken dotted lines in the area t_{eq}. $g_1 = 0.01, g_2 = 0.0025, n\text{th} = 0.08, T = 1, g = 0.05$.

ORCID iD

K V Shulga https://orcid.org/0000-0003-1422-4681

References

[1] Ladd T D, Jelezko F, Laflamme R, Nakamura Y, Monroe C and O'Brien J L 2010 Quantum computers *Nature* **464** 45
[2] Mohamed A-B, Eleuch H and Ooi C H R 2019 Non-locality correlation in two driven qubits inside an open coherent cavity: trace norm distance and maximum bell function *Sci. Rep.* **9** 19632
[3] Govia L, Lingenfelter A and Clerk A 2022 Stabilizing two-qubit entanglement by mimicking a squeezed environment *Phys. Rev. Res.* **4** 023010
[4] Bernien H *et al* 2017 Probing many-body dynamics on a 51-atom quantum simulator *Nature* **551** 579
[5] Akahoshi Y, Maruyama K, Oshima H, Sato S and Fujii K 2023 Partially fault-tolerant quantum computing architecture with error-corrected clifford gates and space-time efficient analog rotations (arXiv:2303.13181)
[6] Moody G *et al* 2022 roadmap on integrated quantum photonics *J. Phys. Photon.* **4** 012501
[7] Krasnok A, Dhakal P, Fedorov A, Frigola P, Kelly M and Kutsaev S 2023 Advancements in superconducting microwave cavities and qubits for quantum information systems (arXiv:2304.09345)
[8] Viola L and Lloyd S 1998 Dynamical suppression of decoherence in two-state quantum systems *Phys. Rev.* A **58** 2733
[9] Zurek W H 2003 Decoherence, einselection and the quantum origins of the classical *Rev. Mod. Phys.* **75** 715
[10] Dittrich T, Hänggi P, Ingold G-L, Kramer B, Schön G and Zwerger W 1998 *Quantum Transport and Dissipation* vol 3 (Wiley-Vch Weinheim)
[11] Grifoni M and Hänggi P 1998 Driven quantum tunneling *Phys. Rep.* **304** 229
[12] Kohler S, Lehmann J and Hänggi P 2005 Driven quantum transport on the nanoscale *Phys. Rep.* **406** 379
[13] Khemani V, Lazarides A, Moessner R and Sondhi S L 2016 Phase structure of driven quantum systems *Phys. Rev. Lett.* **116** 250401
[14] Moessner R and Sondhi S L 2017 Equilibration and order in quantum floquet matter *Nat. Phys.* **13** 424
[15] D'Alessio L and Polkovnikov A 2013 Many-body energy localization transition in periodically driven systems *Ann. Phys., NY* **333** 19
[16] Lazarides A, Das A and Moessner R 2015 Fate of many-body localization under periodic driving *Phys. Rev. Lett.* **115** 030402
[17] Ponte P, Papić Z, Huveneers F and Abanin D A 2015 Many-body localization in periodically driven systems *Phys. Rev. Lett.* **114** 140401
[18] Miroszewski K G A and Sacha K 2018 Time crystal platform: from quasicrystal structures in time to systems with exotic interactions *Phys. Rev. Lett.* **120** 140401
[19] Molignini P, van Nieuwenburg E and Chitra R 2017 Sensing floquet-majorana fermions via heat transfer *Phys. Rev.* B **96** 125144
[20] Ying C *et al* 2022 Floquet prethermal phase protected by U(1) symmetry on a superconducting quantum processor *Phys. Rev.* A **105** 012418
[21] Kyprianidis A *et al* 2021 Observation of a prethermal discrete time crystal *Science* **372** 1192
[22] Zhang J *et al* 2017 Observation of a discrete time crystal *Nature* **543** 217
[23] Choi S *et al* 2017 Observation of discrete time-crystalline order in a disordered dipolar many-body system *Nature* **543** 221
[24] Rovny J, Blum R L and Barrett S E 2018 Observation of discrete-time-crystal signatures in an ordered dipolar many-body system *Phys. Rev. Lett.* **120** 180603
[25] Mi X *et al* 2022 Time-crystalline eigenstate order on a quantum processor *Nature* **601** 531
[26] Shulga K, Vakulchyk I, Nakamura Y, Flach S and Fistul M 2021 Time molecules with periodically driven interacting qubits *Quantum Sci. Technol.* **6** 035012
[27] The code is available at: https://github.com/Kirill-Shulga/Time-Molecule

[28] Hill S and Wootters W K 1997 Entanglement and quantum computation *Phys. Rev. Lett.* **78** 5022
[29] von Neumann J 1929 Quantum mechanics of infinite systems *Z. Phys.* **57** 190
[30] Kronig R d L 1926 On the theory of dispersion of x-rays *Josa* **12** 547
[31] Kramers H A 1927 La diffusion de la lumiere par les atomes *Atti Cong. Intern. Fisica (Trans. of Volta Centenary Congress) Como* **2** 545–57
[32] Kubo R 1957 Statistical-mechanical theory of irreversible processes. I. general theory and simple applications to magnetic and conduction problems *J. Phys. Soc. Japan* **12** 570
[33] Cohen-Tannoudji C, Dupont-Roc J and Grynberg G 1998 *Atom-Photon Interactions: Basic Processes and Applications* (Wiley)
[34] Breuer H-P and Petruccione F 2002 *The Theory of Open Quantum Systems* (Oxford University Press on Demand)